



Churchill, R., Werner, M., Biggs, J. J., & Fagereng, A. (2022). Relative Afterslip Moment Does Not Correlate With Aftershock Productivity: Implications for the Relationship Between Afterslip and Aftershocks. *Geophysical Research Letters*, 49(24), [e2022GL101165].
<https://doi.org/10.1029/2022GL101165>

Publisher's PDF, also known as Version of record

License (if available):
CC BY

Link to published version (if available):
[10.1029/2022GL101165](https://doi.org/10.1029/2022GL101165)

[Link to publication record in Explore Bristol Research](#)
PDF-document

This is the final published version of the article (version of record). It first appeared online via Wiley at <https://doi.org/10.1029/2022GL101165> . Please refer to any applicable terms of use of the publisher.

University of Bristol - Explore Bristol Research

General rights

This document is made available in accordance with publisher policies. Please cite only the published version using the reference above. Full terms of use are available:
<http://www.bristol.ac.uk/red/research-policy/pure/user-guides/ebr-terms/>

Geophysical Research Letters[®]

RESEARCH LETTER

10.1029/2022GL101165

Key Points:

- We test for correlations between key characteristics of afterslip and aftershocks to probe a proposed driving relationship
- Relative afterslip moment does not correlate with aftershock productivity or moment (absolute or relative), decay rate, or b -value
- Relative afterslip moment is not a useful indicator of the likelihood of potentially damaging aftershocks

Supporting Information:

Supporting Information may be found in the online version of this article.

Correspondence to:

R. M. Churchill,
robert.churchill@bristol.ac.uk

Citation:




Churchill, R. M., Werner, M. J., Biggs, J., & Fagereng, Å. (2022). Relative afterslip moment does not correlate with aftershock productivity: Implications for the relationship between afterslip and aftershocks. *Geophysical Research Letters*, 49, e2022GL101165. <https://doi.org/10.1029/2022GL101165>

Received 5 SEP 2022
Accepted 15 DEC 2022

© 2022. The Authors.

This is an open access article under the terms of the [Creative Commons Attribution License](https://creativecommons.org/licenses/by/4.0/), which permits use, distribution and reproduction in any medium, provided the original work is properly cited.

Relative Afterslip Moment Does Not Correlate With Aftershock Productivity: Implications for the Relationship Between Afterslip and Aftershocks

R. M. Churchill¹ , M. J. Werner¹ , J. Biggs¹ , and Å. Fagereng²

¹School of Earth Sciences, University of Bristol, Bristol, UK, ²School of Earth and Environmental Sciences, Cardiff University, Cardiff, UK

Abstract Aseismic afterslip has been proposed to drive aftershock sequences. Both afterslip moment and aftershock number broadly increase with mainshock size, but can vary beyond this scaling. We examine whether relative afterslip moment (afterslip moment/mainshock moment) correlates with several key aftershock sequence characteristics, including aftershock number and cumulative moment (both absolute and relative to mainshock size), seismicity rate change, b -value, and Omori decay exponent. We select $M_w \geq 4.5$ aftershocks for 41 tectonically varied mainshocks with available afterslip models. Against expectation, relative afterslip moment does not correlate with tested aftershock characteristics or background seismicity rate. Furthermore, adding afterslip moment to mainshock moment does not improve predictions of aftershock number. Our findings place useful empirical constraints on the link between afterslip and potentially damaging $M_w \geq 4.5$ aftershocks and raise questions regarding the role afterslip plays in aftershock generation.

Plain Language Summary Large earthquakes may be followed by potentially damaging aftershocks as well as slow fault slip, called afterslip. Previous studies have noted that afterslip and aftershocks spread through space together and decay with time similarly, and therefore suggested that afterslip produces or triggers the aftershocks. As most of this evidence is based on observations of individual cases, we set out to investigate the links between afterslip and aftershocks statistically, using a catalog of 41 moderate to large earthquakes from different geographical settings. When we adjust for the size of the earthquake, we find that more afterslip does not correlate with more aftershocks. We also find that whilst certain characteristics of these aftershock sequences vary (e.g., some decay away more quickly than others), none of these characteristics correlate with how much afterslip occurs. We propose that although afterslip may still influence certain characteristics of aftershock sequences in special cases, overall, it does not yet make sense to include afterslip in models that attempt to predict and model aftershock sequence characteristics.

1. Introduction

Understanding the physical mechanisms that drive aftershock sequences may enable effective forecasting to mitigate their impacts. Aftershock sequences (periods of localized, elevated seismicity rate that follow larger earthquakes) often exhibit considerable spatio-temporal complexity (e.g., Ozawa & Ando, 2021; Ross et al., 2019; van der Elst & Shaw, 2015) and can vary in productivity even after controlling for mainshock size (Dascher-Cousineau et al., 2020; Marsan & Helmstetter, 2017). This complexity and variability poses fundamental questions about the mechanisms driving aftershock sequences, and makes deterministic modeling a challenging prospect. Commonly, probabilistic aftershock models, such as the Epidemic Type Aftershock Sequence (ETAS) model (Ogata, 1988; Ogata & Zhuang, 2006), outperform physics-based models (Hardebeck, 2021; Woessner et al., 2011).

Traditionally, coseismic elasto-static Coulomb stress change is considered as the principal trigger of aftershocks (King et al., 1994; Stein, 1999). However, aftershock models based on coseismic Coulomb stress change, such as Coulomb Rate-and-State (Dieterich, 1994), have shown mixed predictive skill: some models perform comparably to ETAS following certain earthquakes (e.g., Mancini et al., 2019, 2020), but many perform worse (e.g., Cattania et al., 2018; Hardebeck, 2021; Woessner et al., 2011). Shortcomings may be partially caused by modeling uncertainty (Cattania et al., 2014; Hainzl et al., 2010) and a lack of constraints on physical properties (Hardebeck, 2021), including the preseismic stress state (Mildon et al., 2019; Wedmore et al., 2017), but may also be due to the existence of additional aftershock triggering mechanisms.

Multiple mechanisms are capable of redistributing crustal stresses following an earthquake (Freed, 2005; Harris, 1998), including dynamic stress changes (Brodsky & van der Elst, 2014; Hill et al., 1993), secondary stress changes (Marsan, 2005; Meier et al., 2014), pore-fluid phenomena (Bosl & Nur, 2002; Miller, 2020), viscoelastic relaxation (Freed & Lin, 2001; Zhang & Shcherbakov, 2016), and aseismic afterslip: a type of transient, aseismic fault-zone readjustment (Avouac, 2015; Bürgmann, 2018). Afterslip may provide a source of stress redistribution that in some circumstances exceeds that of the mainshock: relative afterslip moment (defined as $M_{rel}^{aslip} = M_o^{aslip} / M_o^{co}$, where M_o^{aslip} is afterslip moment and M_o^{co} is the corresponding coseismic moment) is typically $\sim 10\%$ – 30% , but can exceed 100% (Churchill et al., 2022).

Avouac (2015) stated that “Aseismic afterslip drives aftershocks in general,” which is supported by evidence such as their shared Omori-type (Utsu et al., 1995) decay (Ingleby & Wright, 2017; Wennerberg & Sharp, 1997), observations of spatial correlation and early spatial co-migration (e.g., D’Agostino et al., 2012; Jiang et al., 2021; Kato, 2007; Peng & Zhao, 2009; Ross et al., 2017), and numerical models and frameworks consistent with both behaviors (Helmstetter & Shaw, 2009; Perfettini & Avouac, 2004, 2007; Perfettini et al., 2018). However, afterslip models have considerable uncertainty (Churchill et al., 2022), and previous attempts to include afterslip in Coulomb Rate-and-State models have not concluded that afterslip is the principal aftershock driving mechanism (e.g., Cattania et al., 2015). Until now, the afterslip-aftershock discussion has mostly focused on individual case studies, thus it is timely to synthesize available data sets and systematically test links between afterslip and aftershocks. Although existing evidence generally points to spatio-temporal relationships, investigating the link between afterslip moment and aftershock sequence productivity may provide useful constraints for aftershock forecasting.

We investigate whether relative afterslip moment correlates with: (a) aftershock number, (b) cumulative moment (both of which absolute and relative to an expectation, given the mainshock size), (c) seismicity rate change (SRC), (d) aftershock sequence b -value, and (e) decay exponent p from the modified Omori law (Utsu et al., 1995), for potentially damaging $M_w \geq 4.5$ aftershocks. We also investigate whether coseismic moment, afterslip moment, or their sum best correlate with absolute aftershock number, and whether background seismicity rate correlates with M_{rel}^{aslip} . We select aftershocks from the National Earthquake Information Center (NEIC) global catalog (USGS, 2017), for 41 earthquakes in a range of geographical and tectonic settings, with afterslip models described by Churchill et al. (2022). We develop testable hypotheses and define variables (summarized in Table S1 in Supporting Information S1) in Section 2, outline data and methods in Section 3, and present and discuss results in Sections 4 and 5, respectively. Throughout, the superscripts “aslip,” “ashocks,” and “co” refer to afterslip, cumulative aftershock, and coseismic parameters, respectively. We also use the terms driving and triggering interchangeably, and do not distinguish between the substantial loading of faults to failure (i.e., inducing) and the perturbing of faults that are already close to failure (i.e., triggering).

2. Hypotheses

The generic behavior of aftershock sequences can be described using empirical relationships, which form the backbone of probabilistic models including ETAS. Here, we form simple testable hypotheses that predict how certain aftershock sequence characteristics may deviate from these established laws for higher or lower values of M_{rel}^{aslip} .

2.1. Aftershock Sequence Productivity

The Utsu-Seki scaling law (Utsu, 1970) gives aftershock sequence productivity (n_{exp} , the expected number of aftershocks above a given magnitude) as a function of mainshock magnitude (M_w), an exponent (α), and a constant of proportionality (k):

$$n_{exp} = k10^{\alpha M_w}. \quad (1)$$

Aftershock sequence productivities have been observed to vary beyond this scaling (e.g., Marsan & Helmstetter, 2017), possibly due to factors such as fault dip, lithospheric age, normalized rupture area (Dascher-Cousineau et al., 2020), mainshock depth (Nyffenegger & Frohlich, 2000; Persh & Houston, 2004), seismic coupling (Hainzl et al., 2019), and other physical, background characteristics (Hardebeck, 2021).

We investigate whether M_{rel}^{aslip} correlates with relative aftershock productivity (n_{rel}). We hypothesize that a greater M_{rel}^{aslip} will correspond to a greater n_{rel} , as a greater afterslip moment will impart a greater magnitude and/or volume of stress change (Segall, 2010), thus an increased potential to trigger aftershocks. Conversely, one could argue that a greater M_{rel}^{aslip} would correspond to fewer aftershocks and a lower n_{rel} , as afterslip is indicative of velocity-strengthening fault-zone material (Marone et al., 1991; Perfettini & Avouac, 2004). We define relative aftershock productivity (n_{rel}) as:

$$n_{rel} = \frac{n_{abs}}{n_{exp}}, \quad (2)$$

where n_{abs} and n_{exp} are the absolute and expected productivities (in a specified time window). We evaluate α and k in Section 3.2, and confirm for our data that $\alpha \approx 1.0$ (Hainzl & Marsan, 2008; Yamanaka & Shimazaki, 1990).

Similarly, we expect the relative cumulative moment of the aftershocks ($M_{rel}^{ashocks}$) to correlate with M_{rel}^{aslip} , and we test this. $M_{rel}^{ashocks}$ is defined as:

$$M_{rel}^{ashocks} = \frac{M_o^{ashocks}}{M_o^{co}}, \quad (3)$$

where $M_o^{ashocks}$ is cumulative aftershock moment. However, cumulative aftershock moment may be a less stable characteristic than aftershock number, as it is the sum of randomly sampled moments from a heavy-tailed distribution (Zaliapin et al., 2005).

2.2. Background Rate and Seismicity Rate Change

The Dieterich (1994) framework predicts that aftershock rates are proportional to a given reference seismicity rate. Whether this reference rate is best described by declustered (i.e., background) (e.g., Hainzl & Ogata, 2005) or undeclustered (e.g., Catalli et al., 2008) seismicity is a matter of discussion (Cocco et al., 2010). We use declustered background seismicity rate (B) to make an explicit comparison between spontaneous background earthquakes and our aftershock sequences. The framework thus predicts the total expected number of aftershocks in a sequence (n_{tot}) as a function of reference rate (B), the background stressing rate ($\dot{\tau}_r$) and an imposed stress step (τ):

$$n_{tot} \sim \frac{B}{\dot{\tau}_r} \tau, \quad (4)$$

(Helmstetter & Shaw, 2009; Marsan & Helmstetter, 2017). Noting that this relation may not hold on the scale of entire sequences (Page & van der Elst, 2022), we use a simple measure of SRC to explore how aftershock productivity varies with respect to the background rate. We test whether M_{rel}^{aslip} correlates with SRC. We define SRC as:

$$SRC = \frac{n_{abs}}{B}, \quad (5)$$

where B is the number of background events (above magnitude m) expected in the specified time window (Section 3.1). We hypothesize that a greater M_{rel}^{aslip} will correspond to a greater SRC, as again, a greater afterslip moment will impart a greater magnitude and/or volume of stress change, thus an increased potential to trigger aftershocks.

2.3. Magnitude-Frequency Distribution

The Gutenberg-Richter law (Gutenberg & Richter, 1954) describes the magnitude-frequency distribution of seismicity in a given space-time window. The number of earthquakes (n) above a given magnitude (m) depends on parameters describing productivity (a) and distribution (b):

$$n(m) = 10^{a-bm}. \quad (6)$$

Aftershock sequences may exhibit different b -value distributions to mainshocks and larger-scale catalogs (Godano et al., 2014), possibly implying a physical distinction. We therefore investigate whether M_{rel}^{aslip} correlates with b -value.

We hypothesize that a greater M_{rel}^{aslip} will correspond to a larger number of smaller aftershocks, and hence sequences with higher b -values. High M_{rel}^{aslip} may be associated with fault zones that have a greater proportion of velocity-strengthening material (Marone et al., 1991; Perfettini & Avouac, 2004), and/or greater rheological heterogeneity (Muto et al., 2016; Wei et al., 2013). Compared to a more uniformly velocity-weakening fault zone, these conditions may provide more barriers to large ruptures, requiring a greater number of smaller earthquakes to accommodate slip on numerous isolated velocity-weakening fault patches, thus facilitating a higher b -value. Additionally, afterslip may reload isolated asperities resulting in typically small ($M_w < 4$) repeating earthquakes (Uchida & Bürgmann, 2019).

2.4. Aftershock Sequence Decay

The modified Omori law (Utsu et al., 1995) describes how the rate of aftershocks (R) decays with the elapsed time (t), depending on a constant (K), a characteristic onset time (c), and an exponent (p):

$$R(t) = \frac{K}{(t + c)^p}. \quad (7)$$

The parameter p describes the rate of decay and is typically 0.8–1.2 (Hainzl & Marsan, 2008; Utsu et al., 1995). For afterslip velocity time-series fit to this decay form, p is ~ 0.8 –1.04 (Ingleby & Wright, 2017).

We hypothesize that more slowly decaying afterslip will generate longer aftershock sequences. Unfortunately, due to the lack of constraints on the temporal characteristics of afterslip (Churchill et al., 2022), it is not possible to test this directly. Instead, we use M_{rel}^{aslip} as a proxy, positing that it is difficult to reconcile a quickly decaying aftershock sequence with a high M_{rel}^{aslip} . Thus we test whether M_{rel}^{aslip} correlates with aftershock p , estimated using maximum likelihood (Ogata, 1999).

3. Data and Methods

3.1. Data Sources

We use estimates of relative afterslip moment (M_{rel}^{aslip}) from the compilation by Churchill et al. (2022). We investigate 41 mainshocks (exclusions are explained in Text S1 in Supporting Information S1), with varied mechanisms and a wide geographical distribution, thus are a reasonably representative subset of global $M_w \geq 6.0$ mainshocks. However, there is a selection bias, whereby smaller mainshocks, particularly those with low-moderate M_{rel}^{aslip} , are underrepresented, as their afterslip signal may not reach the detection threshold. There is also uncertainty in these estimates. Churchill et al. (2022) showed that estimates of M_{rel}^{aslip} do not correlate with study duration or start-times as expected, including for different estimates following the same mainshock. Therefore, rather than the specific time-period from each afterslip study, we use a systematic aftershock selection time-period of 18 months, which is in the range of compiled afterslip model durations and the range of apparent aftershock durations (corresponding well to the forecastable period) over our approximate magnitude range (Hainzl et al., 2016). We therefore assume that the given M_{rel}^{aslip} estimates are representative of 18 months of afterslip and discuss the possible implications of this in Section 5.

Whilst regional seismic catalogs include a larger number earthquakes than global catalogs, their magnitude scales may not be directly comparable, and their completeness magnitudes vary. We therefore select $M_w \geq 4.5$ aftershocks from the global NEIC catalog to ensure global quasi-comparability. We calculate the catalog's completeness magnitude (M_c) to be 4.5 by a goodness-of-fit test (Wiemer & Wyss, 2000) with an associated b -value of 1.01, estimated throughout using maximum likelihood (Aki, 1965). Estimates of M_c by alternative approaches (Cao & Gao, 2002; Herrmann & Marzocchi, 2021) are discussed in Text S2 in Supporting Information S1, with all corresponding b -value estimates ~ 1.0 . As catalog completeness varies in space and time (Kagan, 2003), we account for any missing $M_w \geq 4.5$ aftershocks in individual sequences. We estimate M_c for each aftershock sequence, and use the estimated a and b -values to predict the number of aftershocks expected between $M_w 4.5$ and the M_c for the sequence (Text S2 in Supporting Information S1).

3.2. Aftershock Selection and Background Rates

We select aftershock sequences using 2D, 3D, and Nearest Neighbor Declustering (NND) selection methods to mitigate the effect of any one method being susceptible to catalog errors or producing erroneous results. As catalog location errors may be up to tens of kilometres (Kagan, 2003) and likely to have a greater relative impact on aftershocks sequences following smaller mainshocks, we implement a conservative minimum selection length-scale of 30 km in our 2D and 3D methods. We assume catalog origin-time errors are negligible. Methods are explained in greater detail in Texts S3–S5 in Supporting Information S1.

Our 2D aftershock selection method uses empirical scaling relations to define a spatial aftershock zone. This method is 2D as selections are made in map-view and seismicity depth is not considered. This method builds on work by Kagan (2002), who approximated aftershock zones as 2D Gaussian distributions (ellipses) and derived scaling relations for the major- and minor-axis lengths of the ellipse, l_{maj} and l_{min} . We scale l_{maj} and l_{min} with mainshock size and mechanism based on the recent mainshock rupture scaling relations by Thingbaijam et al. (2017) and considering mainshock dip angle from the GCMT catalog (Dziewonski et al., 1981; Ekström et al., 2012). The Thingbaijam et al. (2017) scaling relations provide reasonable approximations of mainshock dimensions and aftershock zone size, even for large subduction earthquakes (Zhang et al., 2020, 2021). For each mainshock, we conduct a broad preliminary search for seismicity within $2l_{\text{maj}}$ of the mainshock epicenter (Figure 1a) and use this to define the average location of seismicity. We then find the orientation of an ellipse (with l_{maj} and l_{min} axis lengths) centered at this location which includes the most earthquakes (Figure 1b), thus defining our aftershock selection zone (Figure 1c, Text S3 in Supporting Information S1).

Our 3D aftershock selection method uses a volume that scales with mainshock size, constructed around the mainshock fault geometry and bounded by a single threshold distance for simplicity. We assume that this distance scales with coseismic moment (as aftershock selection must be independent of afterslip moment to avoid a biased result). We assume that the minimum shear stress that can trigger aftershocks occurs at a distance that scales with $M_o^{1/3}$ from the fault (e.g., Marsan, 2005). As the exact scaling relation would depend on numerous assumptions including slip distribution, rupture scaling, surrounding rheology and threshold triggering stress, we use a conservative estimate that ensures a systematic proportion of aftershocks are selected when working with variable real-world earthquakes. We select all aftershocks within $4 \cdot 10^{-6} M_o^{1/3}$ km of the fault plane (Figure 1d), using fault geometries derived from coseismic slip models in the SRCMOD database (Mai & Thingbaijam, 2014) (Text S4 in Supporting Information S1). This method could not be used for 10 mainshocks which lacked available fault models.

For comparison, we also use the NND algorithm (Baiesi & Paczuski, 2004; Zaliapin & Ben-Zion, 2016), which establishes whether every earthquake in a catalog is dependent or independent, based on a distance (defined in terms of location, time and magnitude) to its nearest neighbor. This allows the classification of fore-, main-, and aftershocks. We use the same parameters as Zaliapin and Ben-Zion (2016), with $M_c = 4.5$. The 2003 $M_w 7.2$ Altai earthquake is identified as an aftershock, and thus omitted here.

The number of aftershocks (n_{abs}) selected by each method are given in Figure 1e. For each mainshock, we define the relative spread as the maximum difference between the number selected by any one method and the median number selected by all methods, divided by the median. Across all mainshocks, this has a median value of 0.23, indicating that aftershock number is generally well-constrained (see examples in Text S6 in Supporting Information S1).

We calculate the Utsu-Seki parameters α and k to be 0.99 (with 95% bounds of 0.92–1.06) and $10^{-5.71}$ by linear regression (using the log-transform of Equation 1) for the 29 $M_w \geq 7.0$ mainshocks (Figure 2a). For lower magnitude mainshocks, the compilation may be biased toward more productive mainshocks and thus we exclude them from our calculation. Our estimates are similar to those obtained by Dascher-Cousineau et al. (2020) for their ($M_c = 4.5$) global study ($\alpha = 1.04$, $k = 10^{-6.17}$). We use our estimates to calculate n_{rel} for the subsequent analysis.

We estimate background seismicity rates using the spatial regions identified in the 2D aftershock selection method. Using the (1979–2019) NEIC catalog, we (a) select the median frequency of earthquakes per calendar year, which naturally removes the quietest and loudest years (Helmstetter & Werner, 2012) and (b) fit inter-event times to a Gamma distribution, assuming that the tail of this distribution represents independent events and can be used to estimate background rate (Hainzl et al., 2006; van Stiphout et al., 2012). Whilst these methods (and the subsequent SRC analysis) are simple compared to more rigorous approaches (e.g., Marsan & Nalbant, 2005; van

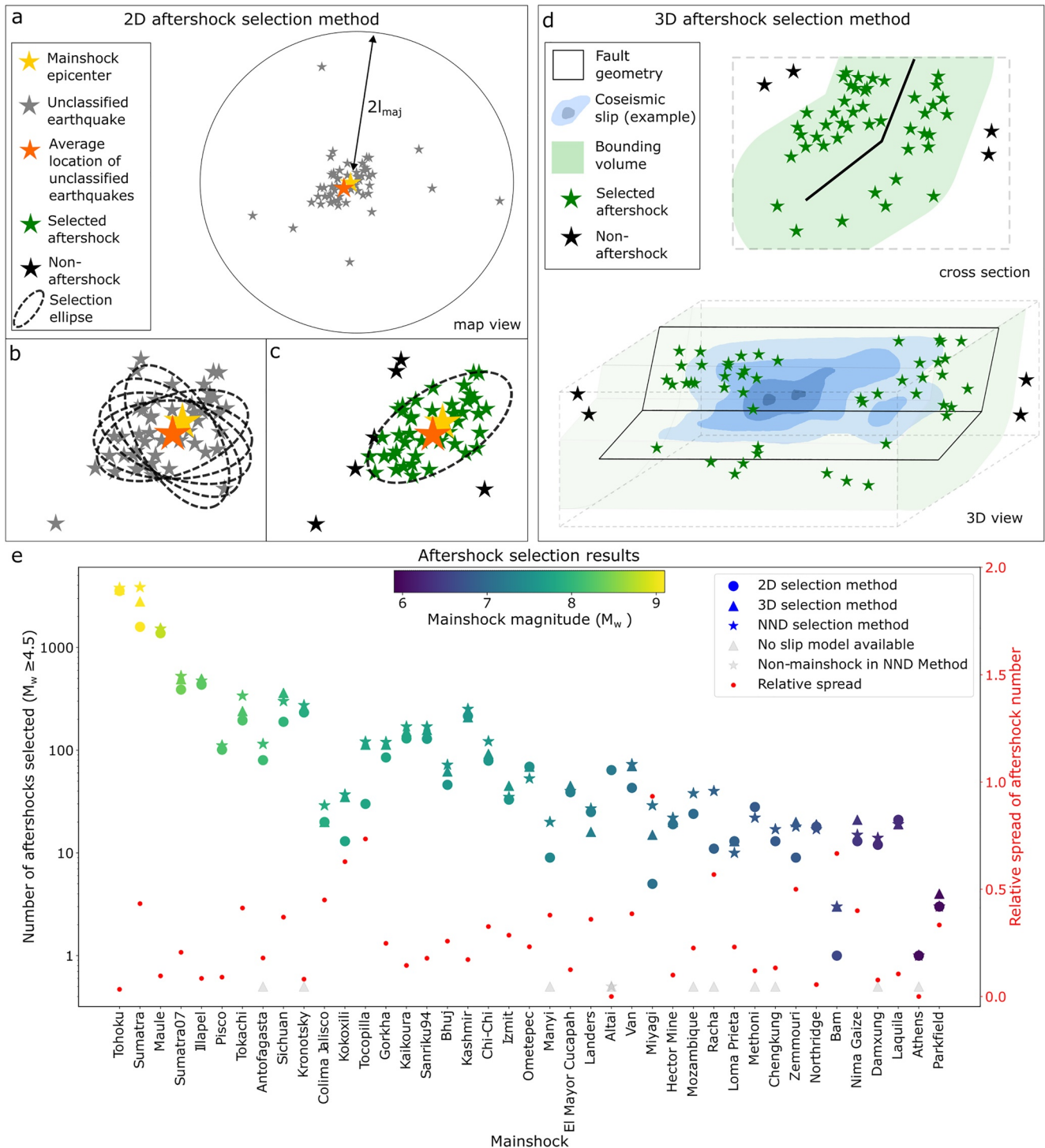


Figure 1. Schematic diagrams of the 2D and 3D aftershock selection methods, and results for all three methods. (a–c) Show a preliminary search for seismicity, fitting the aftershock ellipse, and the selected sequence of the 2D method, (d) shows the 3D aftershock selection method, and (e) shows the number of $M_w \geq 4.5$ aftershocks for each method, for 41 mainshocks ordered by decreasing magnitude. Symbol shape denotes the selection method, color denotes the mainshock magnitude, gray symbols denote where a method was unsuitable (shown above the x-axis), and red circles denote the relative spread of aftershock number estimates for each mainshock. Only one selection method is used for the Altai earthquake.

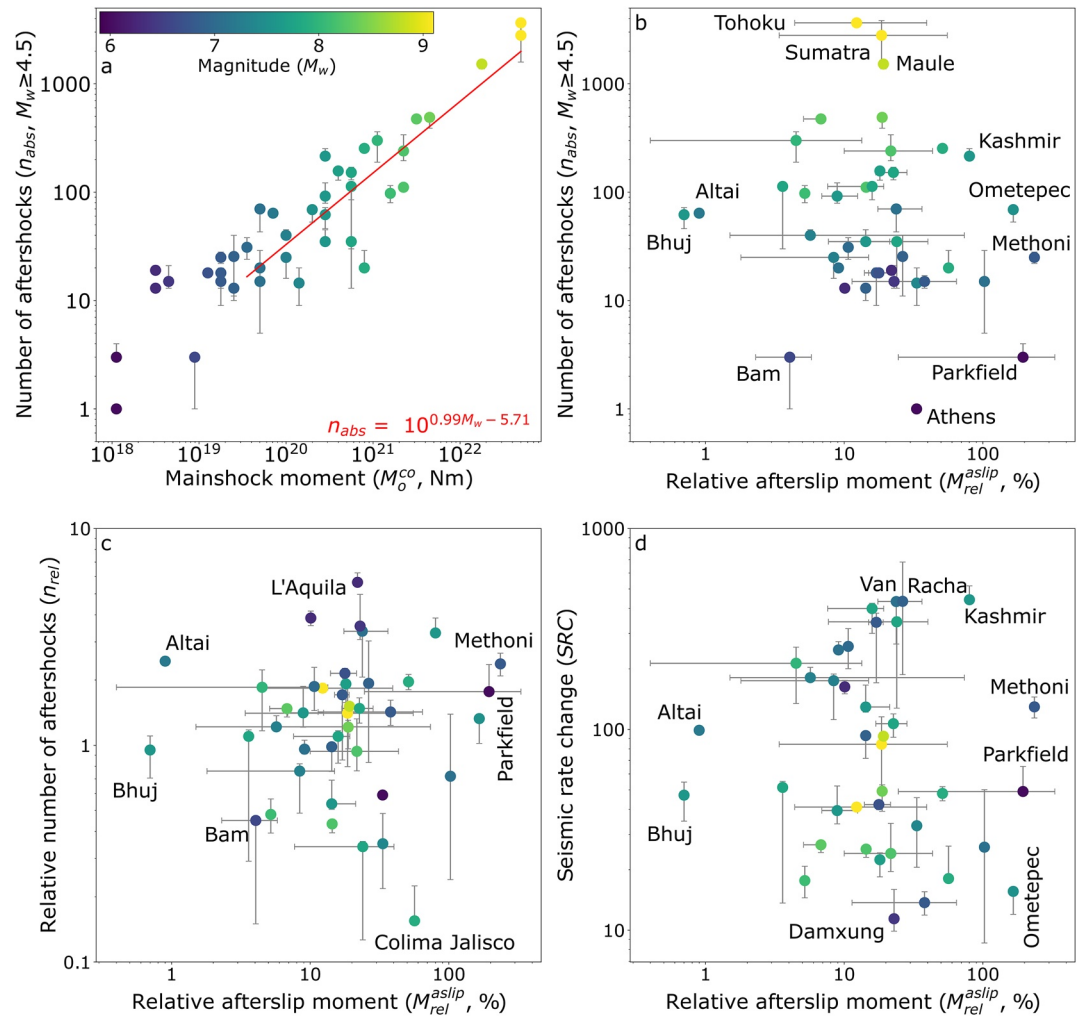


Figure 2. Data showing the strong relationship between coseismic moment and aftershock number and the lack of relationships between relative afterslip moment and key aftershock sequence characteristics: (a) coseismic moment and aftershock number (mainshocks $M_w \geq 7.0$ are fit to Equation 1), (b) relative afterslip moment and aftershock number, (c) relative afterslip moment and relative aftershock number (a factor, see Equation 2), and (d) relative afterslip moment and seismicity rate change (a factor, see Equation 5). Circles denote median values, color denotes mainshock magnitude, gray bars in the y-direction reflect the multiple aftershock selection methods and in the x-direction, reflect multiple estimates of M_{rel}^{aslip} . Endmember mainshocks are annotated.

Stiphout et al., 2011; Zhuang et al., 2005), they are robust and generally produce estimates within a factor of ~ 2 of each other for regions with mainshocks $M_w \geq 7$, but diverge further for $M_w < 7$.

4. Statistical Analysis

We calculate the Spearman's rank correlation coefficient, which tests for monotonic relationships (Dodge, 2008), and/or the gradient (using a first-order least squares inversion), between the characteristics we wish to test. As there are multiple afterslip moment estimates for some earthquakes and up to three aftershock selection methods, we bootstrap to fairly sample data and reflect uncertainty and the range of estimates. For each test, we create 2,000 subsets of randomly sampled data (one data-point per mainshock) and present the median (correlation coefficient or gradient) and 95% range of the resulting distribution. Text S7 in Supporting Information S1 details instances of erroneous, excluded data points in our analyses.

The Spearman's correlation coefficient (median and 95% confidence bounds from bootstrap analysis) between M_o^{co} and n_{abs} is $0.86_{0.82}^{0.90}$. The correlation coefficients between n_{abs} and M_o^{aslip} ($0.73_{0.67}^{0.79}$), and $M_o^{co} + M_o^{aslip}$ ($0.86_{0.81}^{0.90}$)

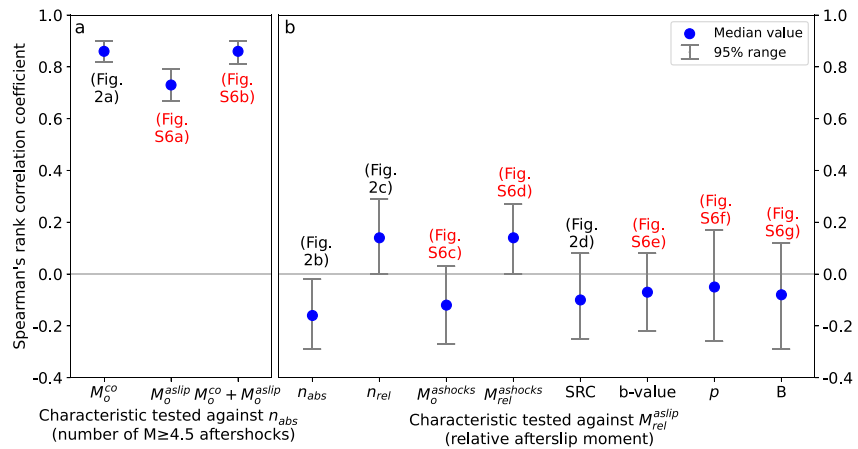


Figure 3. The median Spearman's rank correlation coefficients and 95% bounds of relationships between key characteristics and: (a) n_{abs} and (b) M_{rel}^{aslip} . Forty one mainshocks are analyzed in each case, except for seismicity rate change, b -value, p , and B analyses, which include only 38 mainshocks (Text S7 in Supporting Information S1). Annotations reference the corresponding plots in Figure 2 (black) or Figure S6 in Supporting Information S1 (red).

do not improve on the correlation between M_o^{co} and n_{abs} (Figure 3a). Whilst low magnitude, low M_{rel}^{aslip} mainshocks may be underrepresented in our data set, for these mainshocks $M_o^{co} + M_o^{aslip} \sim M_o^{co}$, thus the relationship will not be significantly affected by the bias.

The estimated correlation coefficients between relative afterslip moment and all key aftershock sequence characteristics tested are $<|0.2|$ (Figure 3b). The median Spearman's correlation coefficients (and 95% bounds) are low between M_{rel}^{aslip} and n_{abs} ($-0.16_{-0.29}^{0.02}$), and between M_{rel}^{aslip} and n_{rel} ($0.14_{0.00}^{0.29}$), with mainshocks existing in all four quadrants (Figures 2b and 2c). Correlation coefficients are also low between M_{rel}^{aslip} and: $M_o^{ashocks}$ ($-0.12_{-0.27}^{0.03}$), $M_{rel}^{ashocks}$ ($0.14_{0.00}^{0.27}$), and SRC ($-0.10_{-0.25}^{0.08}$), with values of SRC varying from ~ 10 to more than 100 times the background rate (Figure 2d). The correlation coefficient between M_{rel}^{aslip} and background seismicity rate is $-0.08_{-0.29}^{0.12}$, implying that B is not a good predictor of M_{rel}^{aslip} . The correlation coefficients between M_{rel}^{aslip} and aftershock b -value ($-0.07_{-0.22}^{0.08}$) and decay exponent p ($-0.05_{-0.26}^{0.17}$) are also low (Figure 3b). Both b -values and p cluster around 1.0 (Figure S6 in Supporting Information S1), which is consistent with previous studies (Shcherbakov et al., 2005; Utsu et al., 1995), with outlying values likely caused by the relatively high M_c .

5. Discussion

For our data set of 41 mainshocks and their $M_w \geq 4.5$ aftershocks, we find no strong relationship between relative afterslip moment and (a) absolute or relative aftershock productivity, (b) absolute or relative cumulative aftershock moment, (c) the SRC, (d) the b -value, or (e) the decay exponent p of the aftershock sequences. The strong correlation between absolute afterslip moment and aftershock productivity can be explained by the scaling of both of these factors with mainshock moment (Churchill et al., 2022; Utsu, 1970). However, the lack of proportionality between relative afterslip moment and relative aftershock number implies they scale differently with mainshock size: Helmstetter et al. (2005) considered aftershock productivity scaling using elasto-static stress transfer between fractally distributed dislocations. We also find that coseismic moment is a better indicator of aftershock sequence productivity than either afterslip moment or the sum of afterslip and coseismic moments. We therefore reject the hypothesis that afterslip is the dominant control on all aftershock sequence characteristics. Despite case study evidence supporting a link, our findings contrast with the concept that afterslip drives aftershocks (e.g., Avouac, 2015; Perfettini et al., 2018). We discuss the role afterslip may play in influencing aftershock sequences alongside other mechanisms and the implications of our findings for seismic hazard analysis.

Several mechanisms, including afterslip, coseismic Coulomb stress change, dynamic triggering, and pore-fluid mechanisms, may be capable of triggering aftershocks and some can explain an Omori-type aftershock decay (Helmstetter & Sornette, 2002; Miller, 2020). Multiple mechanisms may operate simultaneously and their relative importance may be case-specific. For example, Ross et al. (2017) showed that both afterslip and fluid diffusion triggered aftershocks following the 2010 $M_w 7.2$ El Mayor Cucapah earthquake. We can therefore assume that

aftershock triggering is not driven by a single mechanism, and that afterslip plays a varied and non-ubiquitous role in influencing aftershock sequence characteristics (e.g., one could posit that the importance of afterslip in driving aftershocks depends on their respective zones being close together, which may not be the case when afterslip occurs only at depth). This is consistent with our finding that afterslip moment does not universally correlate with key aftershock characteristics and previous evidence supporting case-study links.

In particular, afterslip may influence the spatio-temporal distribution of aftershocks, as is supported by case study observations of early spatio-temporal co-migration of afterslip and aftershocks (Feng et al., 2020; Huang et al., 2017; Jiang et al., 2021; Peng & Zhao, 2009). Whilst we show that aftershock decay rate is not controlled by relative afterslip moment, it could still be influenced by other afterslip characteristics, such as its migration or decay rate. Furthermore, as Page and van der Elst (2022) found that aftershock productivity relates to background seismicity rate at spatially discretized scales within individual sequences, but not at the scale of entire sequences, one could hypothesize that afterslip characteristics drive aftershock sequence productivity at spatially discretized scales within individual aftershock sequences, effectively driving their spatio-temporal distribution. However, our results indicate that relative aftershock productivity may be controlled by other mechanisms and factors such as physical fault-zone and background characteristics, although no single parameter has been shown to dominate (e.g., Dascher-Cousineau et al., 2020; Hainzl et al., 2019; Hardebeck, 2021), indicating that multivariate analysis approaches may be well-suited to investigating this question further.

Limitations in our data and methodology may also obscure relationships. Our relatively high M_c of 4.5 is necessary for ensuring comparability globally, but does not allow us to test the hypothesis that afterslip disproportionately drives smaller aftershocks. As afterslip may drive typically small ($M_w < 4$) repeating earthquakes (Uchida & Bürgmann, 2019), our analysis may be missing relationships involving lower magnitude aftershocks. Uncertainty may also be obscuring weak correlations: Churchill et al. (2022) estimated that uncertainty in afterslip moment estimates is typically a factor of 2–3, and we showed that our aftershock selection methods generate an average relative spread of 23%. Furthermore, the compiled afterslip models have different corresponding modeling time periods, requiring us to use a uniform time-period for aftershock selection, and the data bias may mean that lower magnitude mainshocks, particularly with low M_{rel}^{aslip} , are underrepresented. Additionally, given that considerable variability in aftershock productivity is well-established (e.g., Dascher-Cousineau et al., 2020; Marsan & Helmstetter, 2017), our null result may be because of our relatively small sample size of 41 mainshocks. Therefore, both constraints on the statistical power of our analysis and the previously mentioned sources of uncertainty mean that we cannot reject weak relations between afterslip and aftershocks. However, we argue that if strong relations existed, these would influence the correlation coefficients despite these limitations.

Our results indicate that the standard Utsu-Seki scaling relation (Utsu, 1970) is a more useful indicator of the likelihood of potentially damaging $M_w \geq 4.5$ aftershocks, than when afterslip moment is incorporated. We provide evidence that considering afterslip would not improve probabilistic aftershock hazard forecasts (e.g., ETAS and Coulomb Rate-and-State models), particularly considering the challenges surrounding providing accurate and timely measurements of afterslip (Churchill et al., 2022). However, future work is vital to establish whether specific characteristics of afterslip influence the spatio-temporal distributions of aftershocks, their productivity in special cases, and/or their behaviors below $M_w 4.5$.

6. Conclusion

Whilst some studies claim that afterslip principally drives aftershocks, our results contradict a strong link between relative afterslip moment and several primary ($M_w \geq 4.5$) aftershock sequence characteristics, following 41 global mainshocks. We find that:

1. Aftershock productivity varies between sequences beyond the scaling which is expected with mainshock moment, and beyond the effect of background rate, in contrast to the Dieterich (1994) model.
 2. Relative afterslip moment does not correlate with the key aftershock sequence characteristics tested: aftershock number or cumulative moment (both in absolute or relative terms), SRC, b -value or Omori exponent p .
- We can reject the hypothesis that afterslip moment controls aftershock productivity.

3. Mainshock moment best indicates aftershock sequence productivity. This supports the use of mainshock moment within probabilistic aftershock hazard models (e.g., Field et al., 2017; Wang et al., 2022), although additional characteristics have been linked to variability in aftershock productivity.
4. Characteristics of afterslip may still influence aftershock sequence behaviors in some capacity (their spatio-temporal distributions, productivity in specific cases, behaviors $M_w \leq 4.5$), but further investigation is needed.

Data Availability Statement

Data used are accessible through: Churchill et al. (2022), <https://doi.org/10.5281/zenodo.6414330>, and USGS (2017). Also accessible are our aftershock selection codes: <https://doi.org/10.5281/zenodo.718981> (including our NND catalog), the Omori fitter: <https://github.com/goebel/aftershocks>, b -value/ M_c analysis codes: <https://github.com/sachalapins/bvalues>, and the Lilliefors b -value test: <https://doi.org/10.5281/zenodo.4162497>.

References

- Aki, K. (1965). Maximum likelihood estimate of b in the formula $\log n = a - bm$ and its confidence limits. *Bulletin of the Earthquake Research Institute, University of Tokyo*, 43, 237–239.
- Avouac, J.-P. (2015). From geodetic imaging of seismic and aseismic fault slip to dynamic modeling of the seismic cycle. *Annual Review of Earth and Planetary Sciences*, 43(1), 233–271. <https://doi.org/10.1146/annurev-earth-060614-105302>
- Baiesi, M., & Paczuski, M. (2004). Scale-free networks of earthquakes and aftershocks. *Physical Review*, 69(6), 066106. <https://doi.org/10.1103/physreve.69.066106>
- Bosl, W., & Nur, A. (2002). Aftershocks and pore fluid diffusion following the 1992 landers earthquake. *Journal of Geophysical Research*, 107(B12), ESE 17-1–ESE 17-12. <https://doi.org/10.1029/2001jb000155>
- Brodsky, E. E., & van der Elst, N. J. (2014). The uses of dynamic earthquake triggering. *Annual Review of Earth and Planetary Sciences*, 42(1), 317–339. <https://doi.org/10.1146/annurev-earth-060313-054648>
- Bürgmann, R. (2018). The geophysics, geology and mechanics of slow fault slip. *Earth and Planetary Science Letters*, 495, 112–134. <https://doi.org/10.1016/j.epsl.2018.04.062>
- Cao, A., & Gao, S. S. (2002). Temporal variation of seismic b -values beneath northeastern Japan island arc. *Geophysical Research Letters*, 29(9), 48-1–48-3. <https://doi.org/10.1029/2001gl013775>
- Catalli, F., Cocco, M., Console, R., & Chiaraluca, L. (2008). Modeling seismicity rate changes during the 1997 Umbria-Marche sequence (central Italy) through a rate- and state-dependent model. *Journal of Geophysical Research*, 113(B11), B11301. <https://doi.org/10.1029/2007jb005356>
- Cattania, C., Hainzl, S., Wang, L., Enescu, B., & Roth, F. (2015). Aftershock triggering by postseismic stresses: A study based on Coulomb rate- and state models. *Journal of Geophysical Research: Solid Earth*, 120(4), 2388–2407. <https://doi.org/10.1002/2014jb011500>
- Cattania, C., Hainzl, S., Wang, L., Roth, F., & Enescu, B. (2014). Propagation of Coulomb stress uncertainties in physics-based aftershock models. *Journal of Geophysical Research: Solid Earth*, 119(10), 7846–7864. <https://doi.org/10.1002/2014jb011183>
- Cattania, C., Werner, M. J., Marzocchi, W., Hainzl, S., Rhoades, D., Gerstenberger, M., et al. (2018). The forecasting skill of physics-based seismicity models during the 2010–2012 Canterbury, New Zealand, earthquake sequence. *Seismological Research Letters*, 89(4), 1238–1250. <https://doi.org/10.1785/0220180033>
- Churchill, R., Werner, M., Biggs, J., & Fagereng, Å. (2022). Afterslip moment scaling and variability from a global compilation of estimates. *Journal of Geophysical Research: Solid Earth*, 127(4), e2021JB023897. <https://doi.org/10.1029/2021jb023897>
- Cocco, M., Hainzl, S., Catalli, F., Enescu, B., Lombardi, A., & Woessner, J. (2010). Sensitivity study of forecasted aftershock seismicity based on Coulomb stress calculation and rate- and state-dependent frictional response. *Journal of Geophysical Research*, 115(B5), B05307. <https://doi.org/10.1029/2009jb006838>
- D'Agostino, N., Cheloni, D., Fornaro, G., Giuliani, R., & Reale, D. (2012). Space-time distribution of afterslip following the 2009 L'Aquila earthquake. *Journal of Geophysical Research*, 117(B2), B02402. <https://doi.org/10.1029/2011jb008523>
- Dascher-Cousineau, K., Brodsky, E. E., Lay, T., & Goebel, T. H. (2020). What controls variations in aftershock productivity? *Journal of Geophysical Research: Solid Earth*, 125(2), e2019JB018111. <https://doi.org/10.1029/2019jb018111>
- Dieterich, J. (1994). A constitutive law for rate of earthquake production and its application to earthquake clustering. *Journal of Geophysical Research*, 99(B2), 2601–2618. <https://doi.org/10.1029/93jb02581>
- Dodge, Y. (2008). Spearman rank correlation coefficient. *The concise encyclopedia of statistics* (pp. 502–505). Springer.
- Dziwonski, A., Chou, T.-A., & Woodhouse, J. H. (1981). Determination of earthquake source parameters from waveform data for studies of global and regional seismicity. *Journal of Geophysical Research*, 86(B4), 2825–2852. <https://doi.org/10.1029/jb086ib04p02825>
- Ekström, G., Nettles, M., & Dziwonski, A. (2012). The global CMT project 2004–2010: Centroid-moment tensors for 13,017 earthquakes. *Physics of the Earth and Planetary Interiors*, 200, 1–9. <https://doi.org/10.1016/j.pepi.2012.04.002>
- Feng, W., Samsonov, S., Qiu, Q., Wang, Y., Zhang, P., Li, T., & Zheng, W. (2020). Orthogonal fault rupture and rapid postseismic deformation following 2019 ridgecrest, California, earthquake sequence revealed from geodetic observations. *Geophysical Research Letters*, 47(5), e2019GL086888. <https://doi.org/10.1029/2019gl086888>
- Field, E. H., Milner, K. R., Hardebeck, J. L., Page, M. T., van der Elst, N., Jordan, T. H., et al. (2017). A spatiotemporal clustering model for the third Uniform California Earthquake Rupture Forecast (UCERF3-ETAS): Toward an operational earthquake forecast. *Bulletin of the Seismological Society of America*, 107(3), 1049–1081. <https://doi.org/10.1785/0120160173>
- Freed, A. M. (2005). Earthquake triggering by static, dynamic, and postseismic stress transfer. *Annual Review of Earth and Planetary Sciences*, 33(1), 335–367. <https://doi.org/10.1146/annurev.earth.33.092203.122505>
- Freed, A. M., & Lin, J. (2001). Delayed triggering of the 1999 hector mine earthquake by viscoelastic stress transfer. *Nature*, 411(6834), 180–183. <https://doi.org/10.1038/35075548>
- Godano, C., Lippiello, E., & De Arcangelis, L. (2014). Variability of the b value in the Gutenberg–Richter distribution. *Geophysical Journal International*, 199(3), 1765–1771. <https://doi.org/10.1093/gji/ggu359>

- Gutenberg, B., & Richter, C. F. (1954). *Seismicity of the earth and associated phenomena*. Princeton University Press.
- Hainzl, S., Christophersen, A., Rhoades, D., & Harte, D. (2016). Statistical estimation of the duration of aftershock sequences. *Geophysical Journal International*, 205(2), 1180–1189. <https://doi.org/10.1093/gji/ggw075>
- Hainzl, S., & Marsan, D. (2008). Dependence of the Omori-Utsu law parameters on main shock magnitude: Observations and modeling. *Journal of Geophysical Research*, 113(B10), B10309. <https://doi.org/10.1029/2007jb005492>
- Hainzl, S., & Ogata, Y. (2005). Detecting fluid signals in seismicity data through statistical earthquake modeling. *Journal of Geophysical Research*, 110(B5), B05S07. <https://doi.org/10.1029/2004jb003247>
- Hainzl, S., Scherbaum, F., & Beauval, C. (2006). Estimating background activity based on interevent-time distribution. *Bulletin of the Seismological Society of America*, 96(1), 313–320. <https://doi.org/10.1785/0120050053>
- Hainzl, S., Sippl, C., & Schurr, B. (2019). Linear relationship between aftershock productivity and seismic coupling in the northern Chile subduction zone. *Journal of Geophysical Research: Solid Earth*, 124(8), 8726–8738. <https://doi.org/10.1029/2019jb017764>
- Hainzl, S., Zöller, G., & Wang, R. (2010). Impact of the receiver fault distribution on aftershock activity. *Journal of Geophysical Research*, 115(B5), B05315. <https://doi.org/10.1029/2008jb006224>
- Hardebeck, J. L. (2021). Spatial clustering of aftershocks impacts the performance of physics-based earthquake forecasting models. *Journal of Geophysical Research: Solid Earth*, 126(2), e2020JB020824. <https://doi.org/10.1029/2020jb020824>
- Harris, R. A. (1998). Introduction to special section: Stress triggers, stress shadows, and implications for seismic hazard. *Journal of Geophysical Research*, 103(B10), 24347–24358. <https://doi.org/10.1029/98jb01576>
- Helmstetter, A., Kagan, Y. Y., & Jackson, D. D. (2005). Importance of small earthquakes for stress transfers and earthquake triggering. *Journal of Geophysical Research*, 110(B5), B05S08. <https://doi.org/10.1029/2004jb003286>
- Helmstetter, A., & Shaw, B. E. (2009). Afterslip and aftershocks in the rate-and-state friction law. *Journal of Geophysical Research*, 114(B1), B01308. <https://doi.org/10.1029/2007jb005077>
- Helmstetter, A., & Sornette, D. (2002). Diffusion of epicenters of earthquake aftershocks, Omori's law, and generalized continuous-time random walk models. *Physical Review E*, 66(6), 061104. <https://doi.org/10.1103/physreve.66.061104>
- Helmstetter, A., & Werner, M. J. (2012). Adaptive spatiotemporal smoothing of seismicity for long-term earthquake forecasts in California. *Bulletin of the Seismological Society of America*, 102(6), 2518–2529. <https://doi.org/10.1785/0120120062>
- Herrmann, M., & Marzocchi, W. (2021). Inconsistencies and lurking pitfalls in the magnitude–frequency distribution of high-resolution earthquake catalogs. *Seismological Research Letters*, 92(2A), 909–922. <https://doi.org/10.1785/0220200337>
- Hill, D. P., Reasenber, P., Michael, A., Arabaz, W., Beroza, G., Brumbaugh, D., et al. (1993). Seismicity remotely triggered by the magnitude 7.3 landers, California, earthquake. *Science*, 260(5114), 1617–1623. <https://doi.org/10.1126/science.260.5114.1617>
- Huang, H., Xu, W., Meng, L., Bürgmann, R., & Baez, J. C. (2017). Early aftershocks and afterslip surrounding the 2015 M_w 8.4 illapel rupture. *Earth and Planetary Science Letters*, 457, 282–291. <https://doi.org/10.1016/j.epsl.2016.09.055>
- Ingleby, T., & Wright, T. (2017). Omori-like decay of postseismic velocities following continental earthquakes. *Geophysical Research Letters*, 44(7), 3119–3130. <https://doi.org/10.1002/2017gl072865>
- Jiang, J., Bock, Y., & Klein, E. (2021). Coevolving early afterslip and aftershock signatures of a San Andreas fault rupture. *Science Advances*, 7(15), eabc1606. <https://doi.org/10.1126/sciadv.abc1606>
- Kagan, Y. Y. (2002). Aftershock zone scaling. *Bulletin of the Seismological Society of America*, 92(2), 641–655. <https://doi.org/10.1785/0120010172>
- Kagan, Y. Y. (2003). Accuracy of modern global earthquake catalogs. *Physics of the Earth and Planetary Interiors*, 135(2–3), 173–209. [https://doi.org/10.1016/s0031-9201\(02\)00214-5](https://doi.org/10.1016/s0031-9201(02)00214-5)
- Kato, N. (2007). Expansion of aftershock areas caused by propagating post-seismic sliding. *Geophysical Journal International*, 168(2), 797–808. <https://doi.org/10.1111/j.1365-246x.2006.03255.x>
- King, G. C., Stein, R. S., & Lin, J. (1994). Static stress changes and the triggering of earthquakes. *Bulletin of the Seismological Society of America*, 84(3), 935–953. <https://doi.org/10.1785/BSSA0840030935>
- Mai, P. M., & Thingbaijam, K. (2014). SRCMOD: An online database of finite-fault rupture models. *Seismological Research Letters*, 85(6), 1348–1357. <https://doi.org/10.1785/0220140077>
- Mancini, S., Segou, M., Werner, M., & Cattania, C. (2019). Improving physics-based aftershock forecasts during the 2016–2017 central Italy earthquake cascade. *Journal of Geophysical Research: Solid Earth*, 124(8), 8626–8643. <https://doi.org/10.1029/2019jb017874>
- Mancini, S., Segou, M., Werner, M. J., & Parsons, T. (2020). The predictive skills of elastic Coulomb rate-and-state aftershock forecasts during the 2019 Ridgecrest, California, earthquake sequence. *Bulletin of the Seismological Society of America*, 110(4), 1736–1751. <https://doi.org/10.1785/0120200028>
- Marone, C., Scholtz, C., & Bilham, R. (1991). On the mechanics of earthquake afterslip. *Journal of Geophysical Research*, 96(B5), 8441–8452. <https://doi.org/10.1029/91jb00275>
- Marsan, D. (2005). The role of small earthquakes in redistributing crustal elastic stress. *Geophysical Journal International*, 163(1), 141–151. <https://doi.org/10.1111/j.1365-246x.2005.02700.x>
- Marsan, D., & Helmstetter, A. (2017). How variable is the number of triggered aftershocks? *Journal of Geophysical Research: Solid Earth*, 122(7), 5544–5560. <https://doi.org/10.1002/2016jb013807>
- Marsan, D., & Nalbant, S. S. (2005). Methods for measuring seismicity rate changes: A review and a study of how the M_w 7.3 landers earthquake affected the aftershock sequence of the M_w 6.1 Joshua tree earthquake. *Pure and Applied Geophysics*, 162(6), 1151–1185. <https://doi.org/10.1007/s00024-004-2665-4>
- Meier, M.-A., Werner, M., Woessner, J., & Wiemer, S. (2014). A search for evidence of secondary static stress triggering during the 1992 M_w 7.3 landers, California, earthquake sequence. *Journal of Geophysical Research: Solid Earth*, 119(4), 3354–3370. <https://doi.org/10.1002/2013jb010385>
- Mildon, Z., Roberts, G. P., Faure Walker, J., & Toda, S. (2019). Coulomb pre-stress and fault bends are ignored yet vital factors for earthquake triggering and hazard. *Nature Communications*, 10(1), 1–9. <https://doi.org/10.1038/s41467-019-10520-6>
- Miller, S. A. (2020). Aftershocks are fluid-driven and decay rates controlled by permeability dynamics. *Nature Communications*, 11(1), 1–11. <https://doi.org/10.1038/s41467-020-19590-3>
- Muto, J., Shibasaki, B., Inumata, T., Ito, Y., Ohta, Y., Miura, S., & Nakai, Y. (2016). Heterogeneous rheology controlled postseismic deformation of the 2011 Tohoku-Oki earthquake. *Geophysical Research Letters*, 43(10), 4971–4978. <https://doi.org/10.1002/2016gl068113>
- Nyffenegger, P., & Frohlich, C. (2000). Aftershock occurrence rate decay properties for intermediate and deep earthquake sequences. *Geophysical Research Letters*, 27(8), 1215–1218. <https://doi.org/10.1029/1999gl010371>
- Ogata, Y. (1988). Statistical models for earthquake occurrences and residual analysis for point processes. *Journal of the American Statistical Association*, 83(401), 9–27. <https://doi.org/10.1080/01621459.1988.10478560>

- Ogata, Y. (1999). Seismicity analysis through point-process modeling: A review. Seismicity patterns, their statistical significance and physical meaning (pp. 471–507).
- Ogata, Y., & Zhuang, J. (2006). Space–time etas models and an improved extension. *Tectonophysics*, *413*(1–2), 13–23. <https://doi.org/10.1016/j.tecto.2005.10.016>
- Ozawa, S., & Ando, R. (2021). Mainshock and aftershock sequence simulation in geometrically complex fault zones. *Journal of Geophysical Research: Solid Earth*, *126*(2), e2020JB020865. <https://doi.org/10.1029/2020jb020865>
- Page, M. T., & van der Elst, N. J. (2022). Aftershocks preferentially occur in previously active areas. *The Seismic Record*, *2*(2), 100–106. <https://doi.org/10.1785/0320220005>
- Peng, Z., & Zhao, P. (2009). Migration of early aftershocks following the 2004 Parkfield earthquake. *Nature Geoscience*, *2*(12), 877–881. <https://doi.org/10.1038/ngeo697>
- Perfettini, H., & Avouac, J.-P. (2004). Postseismic relaxation driven by brittle creep: A possible mechanism to reconcile geodetic measurements and the decay rate of aftershocks, application to the Chi-Chi earthquake, Taiwan. *Journal of Geophysical Research*, *109*(B2), B02304. <https://doi.org/10.1029/2003jb002488>
- Perfettini, H., & Avouac, J.-P. (2007). Modeling afterslip and aftershocks following the 1992 landers earthquake. *Journal of Geophysical Research*, *112*(B7), B07409. <https://doi.org/10.1029/2006jb004399>
- Perfettini, H., Frank, W., Marsan, D., & Bouchon, M. (2018). A model of aftershock migration driven by afterslip. *Geophysical Research Letters*, *45*(5), 2283–2293. <https://doi.org/10.1002/2017gl076287>
- Persh, S. E., & Houston, H. (2004). Strongly depth-dependent aftershock production in deep earthquakes. *Bulletin of the Seismological Society of America*, *94*(5), 1808–1816. <https://doi.org/10.1785/012003191>
- Ross, Z. E., Idini, B., Jia, Z., Stephenson, O. L., Zhong, M., Wang, X., et al. (2019). Hierarchical interlocked orthogonal faulting in the 2019 Ridgecrest earthquake sequence. *Science*, *366*(6463), 346–351. <https://doi.org/10.1126/science.aaz0109>
- Ross, Z. E., Rollins, C., Cochran, E. S., Hauksson, E., Avouac, J.-P., & Ben-Zion, Y. (2017). Aftershocks driven by afterslip and fluid pressure sweeping through a fault-fracture mesh. *Geophysical Research Letters*, *44*(16), 8260–8267. <https://doi.org/10.1002/2017gl074634>
- Segall, P. (2010). *Earthquake and volcano deformation*. Princeton University Press.
- Shcherbakov, R., Turcotte, D. L., & Rundle, J. B. (2005). Aftershock statistics. *Pure and Applied Geophysics*, *162*(6), 1051–1076. <https://doi.org/10.1007/s00024-004-2661-8>
- Stein, R. S. (1999). The role of stress transfer in earthquake occurrence. *Nature*, *402*(6762), 605–609. <https://doi.org/10.1038/45144>
- Thingbaijam, K. K. S., Martin Mai, P., & Goda, K. (2017). New empirical earthquake source-scaling laws. *Bulletin of the Seismological Society of America*, *107*(5), 2225–2246. <https://doi.org/10.1785/0120170017>
- Uchida, N., & Bürgmann, R. (2019). Repeating earthquakes. *Annual Review of Earth and Planetary Sciences*, *47*(1), 305–332. <https://doi.org/10.1146/annurev-earth-053018-060119>
- USGS. (2017). *Earthquake hazards program, 2017, preliminary determination of epicenters (PDE) bulletin*. U.S. Geological Survey. <https://doi.org/10.5066/F74T6GJC>
- Utsu, T. (1970). Aftershocks and earthquake statistics (1): Some parameters which characterize an aftershock sequence and their interrelations. *Journal of the Faculty of Science, Hokkaido University. Series 7: Geophysics*, *3*(3), 129–195.
- Utsu, T., Ogata, Y., & Matsu'ura, R. S. (1995). The centenary of the Omori formula for a decay law of aftershock activity. *Journal of Physics of the Earth*, *43*(1), 1–33. <https://doi.org/10.4294/jpe1952.43.1>
- van der Elst, N. J., & Shaw, B. E. (2015). Larger aftershocks happen farther away: Nonseparability of magnitude and spatial distributions of aftershocks. *Geophysical Research Letters*, *42*(14), 5771–5778. <https://doi.org/10.1002/2015gl064734>
- van Stiphout, T., Schorlemmer, D., & Wiemer, S. (2011). The effect of uncertainties on estimates of background seismicity rate. *Bulletin of the Seismological Society of America*, *101*(2), 482–494. <https://doi.org/10.1785/0120090143>
- van Stiphout, T., Zhuang, J., & Marsan, D. (2012). Seismicity declustering, community online resource for statistical seismicity analysis. <https://doi.org/10.5078/corssa-52382934>. Retrieved from <http://www.corssa.org>
- Wang, S., Werner, M. J., & Yu, R. (2022). How well does Poissonian probabilistic seismic hazard assessment (PSHA) approximate the simulated hazard of epidemic-type earthquake sequences? *Bulletin of the Seismological Society of America*, *112*(1), 508–526. <https://doi.org/10.1785/0120210022>
- Wedmore, L., Walker, J. F., Roberts, G. P., Sammonds, P., McCaffrey, K., & Cowie, P. (2017). A 667 year record of coseismic and interseismic Coulomb stress changes in central Italy reveals the role of fault interaction in controlling irregular earthquake recurrence intervals. *Journal of Geophysical Research: Solid Earth*, *122*(7), 5691–5711. <https://doi.org/10.1002/2017jb014054>
- Wei, M., Kaneko, Y., Liu, Y., & McGuire, J. J. (2013). Episodic fault creep events in California controlled by shallow frictional heterogeneity. *Nature Geoscience*, *6*(7), 566–570. <https://doi.org/10.1038/ngeo1835>
- Wennerberg, L., & Sharp, R. V. (1997). Bulk-friction modeling of afterslip and the modified Omori law. *Tectonophysics*, *277*(1–3), 109–136. [https://doi.org/10.1016/S0040-1951\(97\)00081-4](https://doi.org/10.1016/S0040-1951(97)00081-4)
- Wiemer, S., & Wyss, M. (2000). Minimum magnitude of completeness in earthquake catalogs: Examples from Alaska, the western United States, and Japan. *Bulletin of the Seismological Society of America*, *90*(4), 859–869. <https://doi.org/10.1785/0119990114>
- Woessner, J., Hainzl, S., Marzocchi, W., Werner, M., Lombardi, A., Catalli, F., et al. (2011). A retrospective comparative forecast test on the 1992 landers sequence. *Journal of Geophysical Research*, *116*(B5), B05305. <https://doi.org/10.1029/2010jb007846>
- Yamanaka, Y., & Shimazaki, K. (1990). Scaling relationship between the number of aftershocks and the size of the main shock. *Journal of Physics of the Earth*, *38*(4), 305–324. <https://doi.org/10.4294/jpe1952.38.305>
- Zaliapin, I., & Ben-Zion, Y. (2016). A global classification and characterization of earthquake clusters. *Geophysical Journal International*, *207*(1), 608–634. <https://doi.org/10.1093/gji/ggw300>
- Zaliapin, I., Kagan, Y. Y., & Schoenberg, F. P. (2005). Approximating the distribution of Pareto sums. *Pure and Applied Geophysics*, *162*(6), 1187–1228. <https://doi.org/10.1007/s00024-004-2666-3>
- Zhang, L., Goda, K., Werner, M. J., & Tesfamariam, S. (2021). Spatiotemporal seismic hazard and risk assessment of M9.0 megathrust earthquake sequences of wood-frame houses in Victoria, British Columbia, Canada. *Earthquake Engineering & Structural Dynamics*, *50*(1), 6–25. <https://doi.org/10.1002/eqe.3286>

- Zhang, L., Werner, M. J., & Goda, K. (2020). Variability of etas parameters in global subduction zones and applications to mainshock–aftershock hazard assessment variability of etas parameters in global subduction zones and applications to mainshock–aftershock hazard assessment. *Bulletin of the Seismological Society of America*, *110*(1), 191–212. <https://doi.org/10.1785/0120190121>
- Zhang, X., & Shcherbakov, R. (2016). Power-law rheology controls aftershock triggering and decay. *Scientific Reports*, *6*(1), 1–9. <https://doi.org/10.1038/srep36668>
- Zhuang, J., Chang, C.-P., Ogata, Y., & Chen, Y.-I. (2005). A study on the background and clustering seismicity in the Taiwan region by using point process models. *Journal of Geophysical Research*, *110*(B5), B05S18. <https://doi.org/10.1029/2004jb003157>